AAPS PharmSciTech 2007; 8 (3) Article 66 (http://www.aapspharmscitech.org).

An Energy-Based Population-Balance Approach to Model Granule Growth and Breakage in High-Shear Wet Granulation Processes

Received: June 24, 2006; Accepted: March 14, 2007; Published: August 10, 2007

Anish P. Dhanarajan[1] and Rebanta Bandyopadhyay[1]

[1]Michigan Pharmaceutical Sciences, Pfizer Global R&D, Kalamazoo, MI

ABSTRACT

A mathematical model of high shear wet granulation is proposed, where granule breakage, and not growth, is the dominant process. The energy required for granule breakage is assumed to be provided by the impact of granules between themselves and the granulator parts, and the extent of granule breakage determined by the balance between the impact-energy and the work of adhesion between the agglomerating particles. A specific volume of dry powder per unit crack surface area was allowed to reattach to the surface of broken granules to account for granule growth. To verify proposed model conditions, lactose monohydrate was granulated with a relatively low amount (6%) of the binder phase, polyvinylpyrrolidone and water, and was added to the powder before granulation.

The trend in granule size distribution during the experiment closely followed the predicted model with an initial increase in the weight fraction of the larger granules. This increase was possibly due to extensive breakage of weaker granules and less extensive breakage, as if by attrition, of stronger granules, accompanied by the attachment of dry powder to the cracked surfaces. Eventually, larger granules experience increased impact energy and break. When excess binder is added and, higher volumes of powder reattach to the crack surface, more large granules form leading to granule overgrowth. This model highlights the importance of the probability of impact per unit time interval (ie, the rate of impact), the strength of the granules and the volume of powder that could attach to the cracked surface in high shear granulation processes where significant granule breakage is encountered.

KEYWORDS: High shear granulation, population balance, model, granule breakage.

Corresponding Author: Rebanta Bandyopadhyay, Discovery Research, Dr. Reddy's Laboratories, Ltd, Bollaram Road, Miyapur, Hyderabad 500 049, AP, India. Tel: 91 40 2304 5439 (ext 447); Fax: 91 40 2304 5438; E-mail: rebantab@drreddys.com

INTRODUCTION

High-shear wet granulation (HSG) is a fast, efficient, and commonly used batch process in the pharmaceutical industry that offers the advantage of 1-step mixing and granulation. In HSG, a powder mixture undergoes controlled aggregation by agitation with rotating impeller(s) typically in the presence of a liquid "binder" phase. The liquid phase could be added all at once or be sprayed continuously over the powder bed during the process. Granulation is thought to occur in successive steps of primary particle nucleation followed by aggregation and breakage due to impact.[1]

Various models of HSG have been proposed to assist in describing, controlling, and scaling-up of the process.[2-9] Such models include primary and derived factors, such as impeller tip speed, relative swept volume, and dimensionless number relationships involving process power consumption. Other scale-up strategies include in situ monitoring of equipment or material properties, design of experiments (DOE), and statistical analysis.

More recently, the "population balance" approach has gained increasing popularity for modeling HSG processes[9-16] in which the total powder mass is distributed among various discrete granule sizes according to predetermined rates of granule growth and breakage.. However, the population balance approach, by itself, lacks the tools to independently predict such kinetics of granule growth and breakage and usually relies on the rate constants obtained from empirical data. Separate rate constants for such individual processes as wetting, nucleation, growth, consolidation, and breakage[4] are sometimes used to improve the overall match between the predicted and observed results.[17] According to Wauters et al,[10] promising results are obtained for granule size predictions in the coalescence and granule growth phases; however, improvements in the area of granule nucleation are necessary. Also, according to Litster and Ennis,[18] there is limited quantitative information in the literature about the effect of granule breakage on granulation.

In order to increase our understanding of the effect of granule breakage under the conditions of mixing employed inside a granulator, a simple model for HSG is proposed and tested, where granule breakage is dominant over granule growth.

Proposed Model

Theory

Particle breakage has been extensively modeled in the comminution literature, where various energy-based breakage models have been introduced.[19,20] The model developed in this study uses an "energy-based breakage principle," where the extent of granule breakage is assumed to depend on the energies of impact of the granules between themselves and the granular parts, such as impellers and chopper during intense mixing inside the granulator bowl. According to this model, the extent of cracking (ie, the new crack surface area generated under impact) is directly proportional to the kinetic energy of the impacting granule and inversely proportional to the strength of the granule. The kinetic energy at impact is, in turn, influenced by the mass and velocity of the impacting granule(s). The binder-rich surfaces exposed on the broken granules and fragments reattach particles and granules, thereby distributing the binder across the powder bed and promoting granule growth, which continues to alter the granule size distribution until the granules are too small to possess enough kinetic energy at impact for breakage. While each broken fragment containing the exposed binder phase is capable of reattachment and growth, granule *breakage* and not growth is expected to be the dominating rate process when the sizes (masses) of the colliding granules are large, the kinetic energy at impact is high, and there is excess dry powder in the granulator. Figure 1 is a schematic representation of the proposed modes of granule breakage and growth.

A list of definitions and assumptions incorporated in the current model follows:

1. Granules are defined as aggregates of particulate material (primary particles) held together by the "binder" phase(s), which could crack and fragment due to their impact (kinetic energy) with other particulates and the granulator parts. Breakage of primary particles is not considered.
2. Only discretized granule size sets are allowed.
3. All collisions are considered to be elastic, and crack propagation is modeled according to the Griffith criterion.
4. Every impact that allows crack propagation is associated with fragmentation (ie, progressive crack propagation over multiple impacts is not considered).
5. Granules are homogeneous in composition and shape. This implies that all broken fragments are of the same shape as the mother granule. Although the shape has been assumed to be spherical in these simulations, other shapes may also be assumed provided an appropriate shape factor (a) is chosen.
6. Granule density is uniform and independent of granule size.
7. The total new crack surface area (ΔS_i) generated by the cracking of each granule is limited to $\Delta S_{i\text{critical}}$, which is the maximum area of new crack surface possible for the size class i under the impact conditions within the granulator.
8. Since kinetic energy is proportional to mass, the value of $\Delta S_{\text{critical}}$ is also proportional to granule mass.
9. The value of $\Delta S_{\text{critical}}$ is also inversely proportional to granule strength or its resistance to cracking. Hence, if desired, the value of $\Delta S_{\text{critical}}$ could be scaled in proportion to some measure of granule strength across various granule compositions.
10. All new crack surfaces are assumed equally capable of attaching primary particles.
11. A fixed volume of dry powder (β) attaches to every unit area of new crack surface generated by impact breakage regardless of the size of the granule. The amount and thickness of the binder layer is not considered to influence its "binding ability."
12. There exists a probability P_i that a granule belonging to a size class "i" will undergo breakage within a time interval Δt. The value of P is considered to be proportional to the projected area of the particle.
13. Reattachment of granules to granules is neglected at this time. This assumption is valid when the amount of binder is limited and the volume of dry powder is significantly greater than the volume of the wet granules.
14. The model is applicable regardless of the precise flow or collision patterns inside the granulator.
15. The rate of breakage is assumed to be a first order rate constant akin to the probability of impact for a given size class of granules.

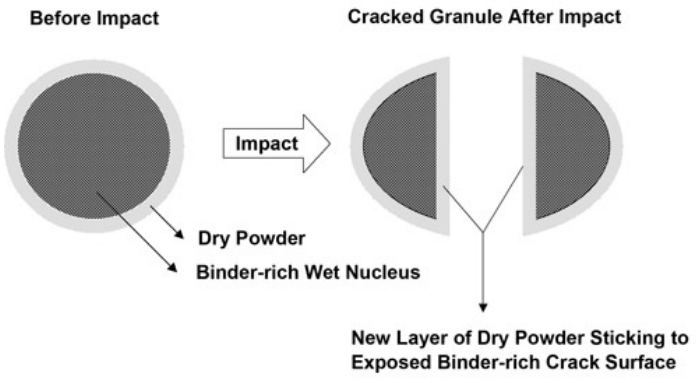

Figure 1. A schematic representation of granule breakage under impact and limited regrowth by the attachment of dry powder to the exposed surfaces. Note that representation of the broken fragments in the Figure is for illustration purposes only and does not reflect the assumption in the model that all broken fragments are of the same shape as the intact granule.

Model Equations

Material balance or the conservation of volume is provided by the following relationship in Equation 1.

$$v^i = \sum_j n_j v_j^{i+1}, \tag{1}$$

where v^i is the volume of the unbroken granule in the ith iteration, v_j^{i+1} is the volume of the broken granules of size j in the $(i+1)$th iteration, and n_j is the number of granules of size j. The index j represents the discretized granule sizes.

The change in surface area, which is equivalent to the new crack surface area generated under impact, is calculated from the volume of the initial granule and those of the subsequent fragmented granules formed after breakage as

$$\Delta S = a\left[\sum_j n_j \left(v_j^{i+1}\right)^{2/3} - \left(v^i\right)^{2/3}\right] \tag{2}$$

Since the granules and particles were assumed to be spherical in these simulations, the shape factor "a" assumes the value $\sqrt[3]{36\pi}$. The growth in granule size due to reattachment of dry powder is calculated by the following relationship:

$$\overline{v_j^{i+1}} = v_j^{i+1} + \beta \Delta S \frac{a\left(v_j^{i+1}\right)^{2/3}}{\Delta S + a\left(v^i\right)^{2/3}}, \tag{3}$$

where $\bar{v}$ represents the increased volume after attachment of dry powder on the cracked surface. The parameter β denotes the volume of dry powder that attaches per unit crack surface area (ΔS) exposed from breakage of a granule and has the dimension of length. Equation 3 assumes that the binder-rich surfaces are distributed across the surfaces of the fragmented granules in proportion to the surface area of the fragments.

Experimental Methods

Model Simulation

Simulations were run using the MATLAB programming environment. A discretized set of 10 granule sizes (Table 1) was considered for the simulation. More specifically, i = 1, 2, 3, … 10 in Equation 1, where the number 10 represents the largest particle size. The granule size, expressed as granule diameter, is a nondimensional number and may assume any value or unit when scaled with an appropriate factor. The fragment-size distributions upon breakage of a granule are compliant with Equation 1 which is a material balance constraint.

Table 1. List of discretized particle sizes used in the simulation and the sieve sizes used in the experiments indicating the large, intermediate, and small size ranges.*

Size Class	Simulation†	Experiment‡
Large	7.254	≥3.35 mm
	5.759	
	4.572	
	3.630	
	2.881	
Intermediate	2.287	<3.35 mm,
	1.816	≥0.6 mm
Small	1.442	<0.6 mm
	1.145	
	0.794	

*Data from Wehrlé et al.[2]

†Granule sizes are expressed as nondimensional numbers and may assume any value or unit when scaled with an appropriate factor.

‡A sieve-size opening of 3.35 mm corresponds to mesh No. 6 and that of 0.6 mm corresponds to mesh No. 30.

According to the model hypothesis, only distributions that satisfy the condition

$$\Delta S \le \Delta S_{critical}, \tag{4}$$

are allowed breakages and each of the allowed distributions is assumed to have equal probability of occurrence in the simulation. The following steps are performed to determine the average number of particles of size class "i" that is formed due to the breakage of a parent granule of size class "j":

1. The set of all distributions $\{n_i\}$ that are in compliance with Equation 1 are computed.
2. From the entire set, only the distributions that satisfy the energy criteria $\Delta S_i \le \Delta S_{i\text{critical}}$ are selected.
3. Since each of the distributions selected from step (2) is equally likely to occur, the number of fragments of class "i" that is formed by the breakage of the parent particle is determined by the average number of particles of a size class "i" across all the "allowed" distributions.
4. Granule regrowth, as defined by Equation 3, is then calculated for each allowed granule fragment.

Step (4) yields a large number of particles between any 2 size ranges "i" and "i+1". An increase in the number of iterations leads to a geometric increase in the number of particles in the simulation. Consequently, to reduce computation effort, the granule sizes were readjusted after each iteration to conform to the discrete set adopted for the simulation. This was achieved by equating the total mass of particles between sizes "i" and "i+1", and expressing it in terms of the mass (and the number of particles) of an average size of "i" and "i+1".

The probability of breakage, P, and $\Delta S_{critical}$ were assigned values only for the largest size class in the simulations. The P and $\Delta S_{critical}$ values for other size classes were scaled linearly with respect to the projected granule area and the granule volume, respectively. The assignment of values for P and $\Delta S_{critical}$ of the largest size class were made such that the model predictions yielded order of magnitude fits with experimental data. Since $\Delta S_{critical}$ is influenced by the mass of the impacting granule, the scaling to granule volume assumes no densification across the various granule sizes.

At present, the predictions of this model are only applicable when the fraction of the dry powder is relatively high in the granulator. Nevertheless, at the expense of additional computational time and resources, the current model can be modified to incorporate the various binder-related parameters based on previously published studies of the influence of flux rate of the binder on granule growth.[5,21,22]

Materials

All experimental granulation batches were run with modified, spray-dried lactose monohydrate (316 NF Fast Flo lactose) obtained from Foremost Farms (Baraboo, WI), Povidone (polyvinylpyrrolidone [PVP], K-value 30; Plasdone C-30, ISP Corporation, Wayne, NJ) and FD&C red food dye (McCormic and Co, Hunt Valley, MD) in a 250-mL granulator (MiPro, ProCepT nv, Zelzate, Belgium) with impeller and chopper speed set at 200 and 600 rpm, respectively. The binder used was a 25% (wt/vol) solution of PVP with 1% red dye. The red dye was used to track the distribution of the binder in the powder mixture and in the granules.

Granulation

For each run, 47 g lactose was weighed into the granulator bowl and the binder solution was added as 3 boluses (1 mL each) using a syringe (1 cc, Tuberculin, Becton-Dickinson, Franklin Lakes, NJ) to 3 consistent spots on the lactose in the granulator bowl. This step was followed by a waiting time of 10 seconds to allow the binder solution to percolate through the powder bed and form 3 large lumps of aggregated powder. The impeller and the chopper motors were started simultaneously, and the powder bed was mixed for various predetermined time periods as according to the experimental plan, and up to a maximum of 300 seconds. At the end of each run, the powder was carefully collected and spread out on a tray to dry in the open and under ambient temperature conditions (20ºC-25ºC) for 24 hours. Prior to analysis, the dried mass was then gently delumped using a motor-driven mixer attached with a 3-blade impeller that was set to run at 60 rpm inside the bed of granules. Preliminary trials suggested that 60 rpm was the minimum speed setting for the motor at which the impeller could smoothly rotate inside the powder mass without generating unnecessary stresses and attrition due to a stop and go (jerky) motion of the impeller. This step was included to break weak cakes that are formed during the drying step, which could confound the sieve analysis results. The experiments were performed in triplicate.

Size Analysis by Sieving

Following delumping of the granulated powder, sieve-size analysis of the granulation was performed using the sieves listed in Table 1. A Gilsonic sonic sifter (Gilson Co Inc, Lewis Center, OH) was run for 12 seconds at 30% maximum power. The sieves were tared prior to sieving, and the weight of granules collected on each sieve, measured. The larger granules, size greater than or equal to sieve number 16, were sieved manually in larger sieves. A fixed number of taps and rotations were used to completely separate the larger sieve fractions that might not have been possible using a low amplitude sonic shifter. Automated shifting and rigorous shaking was avoided to prevent the dry powder from separating out from the larger granules during sieve analysis.

Results and Discussion

The granule size distributions from typical simulation runs over various times are depicted in Figure 2. As the iterations progress, the larger granules break into smaller granules that tend to cluster toward a final size, below which there is insufficient kinetic energy to break apart the granules. This final size is influenced by the value of $\Delta S_{critical}$, P, and β selected for the simulation run. The impact of $\Delta S_{critical}$ on the granule size distribution after 300 seconds

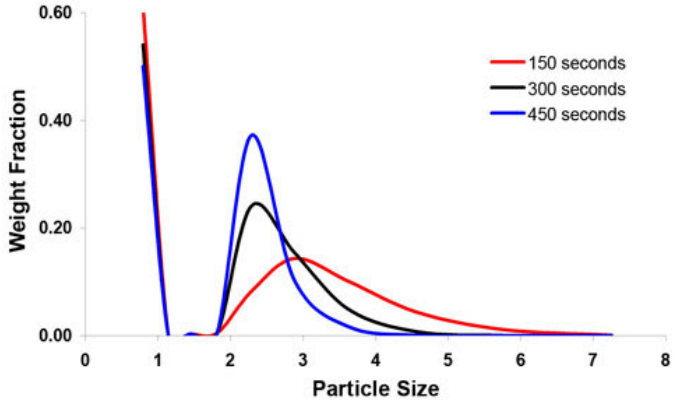

Figure 2. Simulated particle size distributions after different run times (red = 150 seconds, black = 300 seconds, blue = 450 seconds). The values of the other parameters were $\beta = 0.15$, $P_i = 0.025$, and $\Delta S_{critical} / S_i = 0.7$. Initial dry powder weight fraction for the simulations was chosen as 0.75.

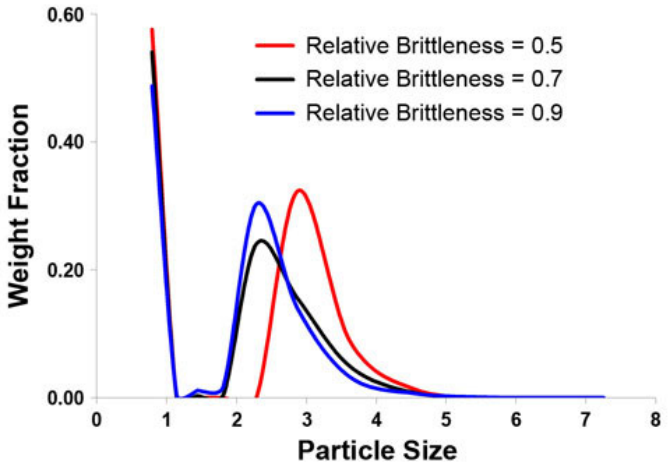

Figure 3. Simulated particle size distributions for various relative brittleness (tendency to fracture into finer fragments) expressed as different values of $\Delta S_{critical}$ /S_i (red = 0.5, black = 0.7, blue = 0.9) for a total granulation time of 300 seconds. The values of the other parameters were: $\beta = 0.15$, $P_i = 0.025$. Initial dry powder weight fraction for the simulations was chosen as 0.75.

is demonstrated in Figure 3. High values of $\Delta S_{critical}$ correspond to greater crack surface area upon impact and represent weaker granules and/or more severe mixing conditions. Consequently, the final mean granule size tends to be smaller than that for smaller values of $\Delta S_{critical}$. Also, since more new crack surface area is exposed upon breakage of the granules at higher values of $\Delta S_{critical}$, the rate and extent of consumption of dry powder is increased.

In the actual granulation experiments, the breakage of granule and the redistribution of the binder were tracked using the color change in various granule size fractions over time. As illustrated in Figure 4, at the start of the granulation experiments, where the red-dyed binder solution was dumped into the powder bed, the red pigment was associated with the largest of the granules formed by the lumping of the powder mass that was directly in contact with the added binder solution. Over the course of the granulation run, however, more and more smaller granules were generated from the breakage of the larger masses as indicated by their color. The volume of primary powder particles (lactose) that ranged in size up to ~180 μm gradually depleted over time, possibly owing to sticking to the binder-rich surfaces of the broken granule fragments. Under the conditions of the experiments, the dry powder was in excess and quickly coated the exposed, binder-rich surfaces of the broken fragments and, hence, the reattachment of granules to other granules was expected to be rare.

The effect of various simulation parameters on the time profiles of 3 broad granule size ranges, small, intermediate, and large are depicted in Figures 5-7. By combining the various sieve-cuts and simulation sizes (Table 1) into these 3 broad size classes, the evolution of the granule size distribution is illustrated over time. At the start of a simulation, finite weight fractions were assigned to the appropriate discrete size classes based on the weight fractions observed at time $t = 0$ of actual experimental batches, after adding the binder phase. Figure 5 demonstrates the effects of low, intermediate, and high $\Delta S_{critical}$ on the weight fraction of each of the size classes (large, intermediate, small) over time. The dimensionless values of $\Delta S_{critical}$ for this simulation are expressed relative to the surface area S_i of the largest discrete granule size. For high $\Delta S_{critical}/S_i$ values representing weaker granules, breakage of the granules is quicker leading to the faster decline in the weight fraction of the smaller size class comprising the dry powder particles, as more broken surfaces are available for their attachment. The weight fraction of the larger size class increases initially due to regrowth from powder attachment but declines over time as more large granules break up. For obvious reasons, the decline in the weight fraction of the larger size class is accompanied with a gradual increase in the intermediate sizes. For the strongest of the granules simulated ($\Delta S_{icritical}/S_i = 0.5$), the

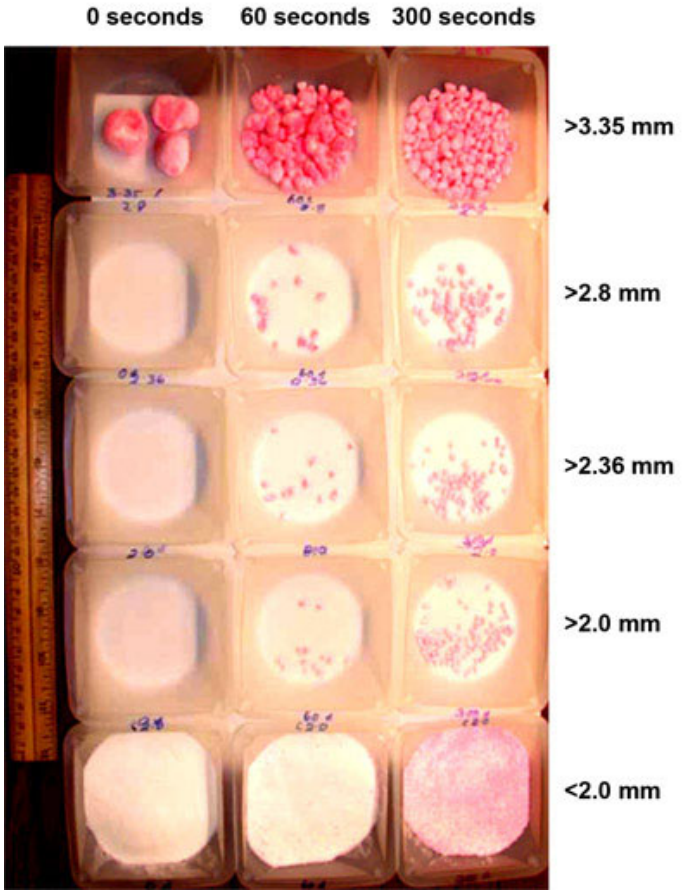

Figure 4. Photographs of various granule sizes evolving over time (0, 60, and 300 seconds) during a granulation process and the distribution of the binder depicted by the spreading of the red pigment.

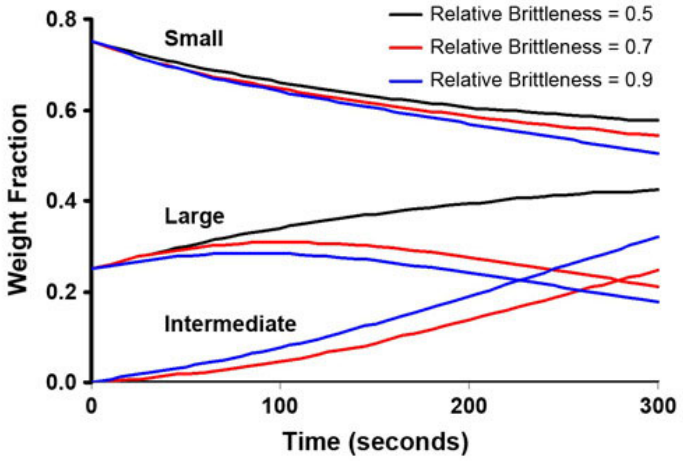

Figure 5. Simulated time profiles of small, large, and intermediate granules for 3 values of $\Delta S_{critical}/S_i$ (red = 0.5, black = 0.7, blue = 0.9); initial dry powder weight fraction = 0.75, while $\beta = 0.15$, and $P_i = 0.025$.

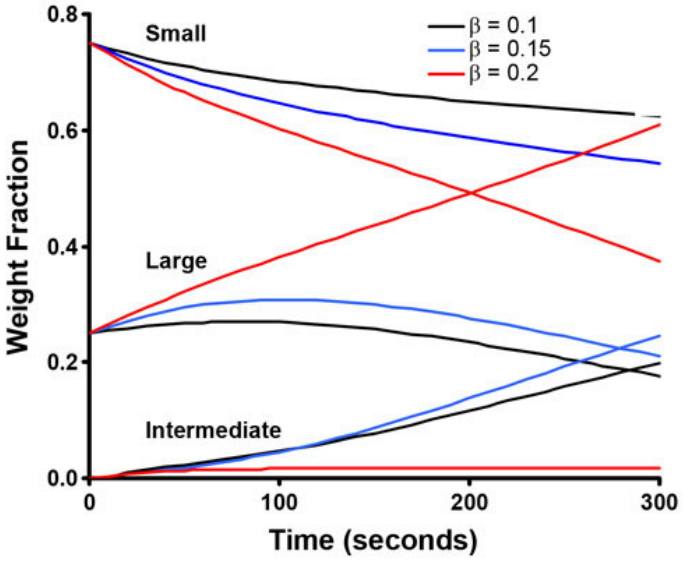

Figure 6. Simulated time profiles of small, large, and intermediate granules for 3 values of β (red = 0.10, black = 0.15, blue = 0.20); initial dry powder weight fraction = 0.75, while $\Delta S_{critical}/S_i = 0.7$, and $P_i = 0.025$.

larger granules undergo minimal breakage, as if in attrition, and consequently, the attachment of powder to the crack surfaces leads to an overall increase in the weight fractions of the larger sizes. Within the time span of the simulations in Figure 5, no intermediate size granules are formed. Figure 6 demonstrates the effects of low, intermediate, and high β on the weight fraction of each of the size classes (large, intermediate, small) over time. As intuitively expected, for higher values of β, more dry powder attaches to the broken surfaces and, hence, there is faster decline of the small particle weight fraction within the granulator. For the highest value of β used in the study simulations (β = 0.20), more granules end up in the largest size class due to regrowth, and almost no increase in the number (and weight fraction) of the intermediate-sized granules is observed. Since P is defined as the probability of granule breakage within the time interval Δt, an increase in probability is otherwise equivalent to a corresponding increase in granulation time. A relative increase in P results in a faster decline in the small and large granules and in a quicker increase in the number (and weight fraction) of intermediate-sized granules (Figure 7).

The trends reflected in the experimental results correspond with the model simulations, as shown by the overlayed predictions (Figure 8). The "small" size range is composed of the particles of lactose monohydrate (mostly less than 180 μm). The weight fraction of the small size class undergoes a sharp decline followed by a gradually flat profile indicating that the breakage of the granules or the exposure of binder-rich surfaces is stopped after a certain intermediate granule size is attained. The weight fraction of granules in the intermediate size class increases with time and then stays constant because of the inability of the granulator to break up the granules any further (Figure 8). An initial lag time that appears in the time profile of the intermediate-sized particles corresponds to the time required for the larger granules to break and for the broken granules to start appearing in this intermediate size range.

In the presence of excess binder, or if the overall rate at which the sticky surfaces are created and exposed exceeds the rate at which the dry powder can attach, more wet (sticky) surfaces could be introduced leading to the agglomeration of multiple granules into bigger "nuggets." This phenomenon of granule "overgrowth" by granule-granule sticking is not

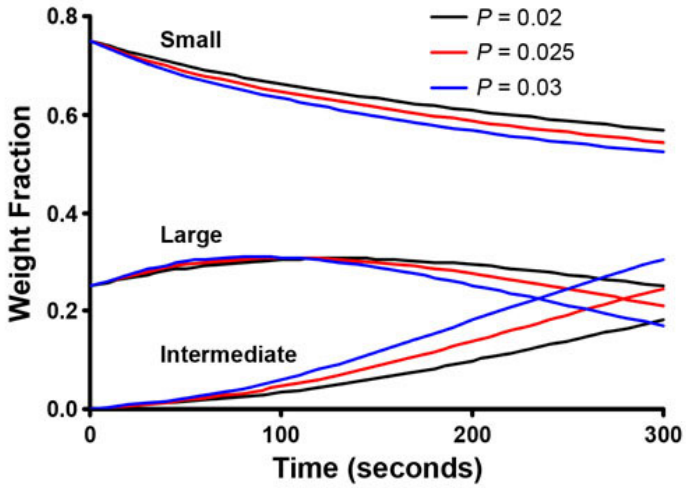

Figure 7. Simulated time profiles of small, large, and intermediate granules for 3 values of P_i (red = 0.020, black = 0.025, blue = 0.030); initial dry powder weight fraction = 0.75, while $\Delta S_{critical}/S_i = 0.7$, and $\beta = 0.15$.

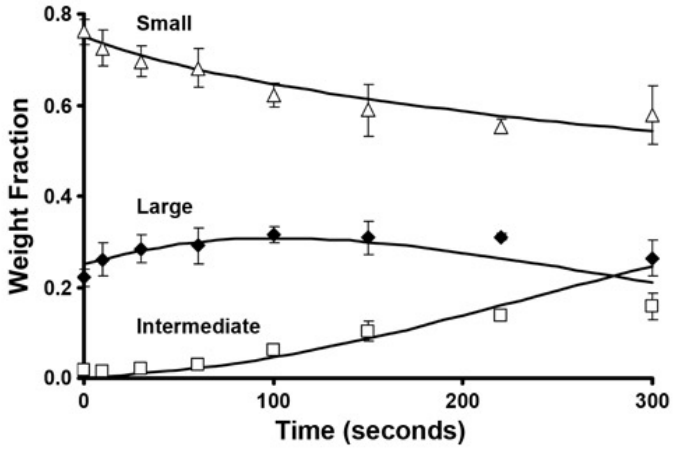

Figure 8. Experimental (data points) and simulated (lines) time profiles of small (Δ), large (♦), and intermediate (□) granules. $\Delta S_{critical}/S_i = 0.7$; $\beta = 0.15$, P_i 0.025; initial dry powder weight fraction = 0.75.

accounted for by the calculated simulations at this time. In these experiments, the dry powder fraction is relatively high compared with the binder phase; further extension of the model is necessary to account for over-wetting, when growth due to granule-granule adhesion or coalescence becomes significant. Information about the spray pattern, the area of the powder bed directly wetted by the spray, and the spray droplet size distribution could also be used in the future to account for the influence of binder spray in the existing model. Also, the viscous dissipation forces in the presence of the binder liquid, various spray conditions that are employed for binder addition, and the variegated mechanical properties of the components of an actual formulation would further complicate the fracture behavior of granules. The possibility of reattachment of the cracked granules amongst themselves will be added to future models to account for those experimental situations, where there is excess of binder in proportion to the dry powder mass or when the binder is introduced as a fine enough spray such that the nuclei formed by the powder particles sticking to the binder droplets are too small in size (mass) to experience sufficient kinetic energy at impact to break.

In spite of its apparent simplicity, the proposed model provides a unique, fairly accurate, and easily applicable tool to predict the granule size distribution in HSG processes when significant granule breakage is encountered. The "energy-based granule breakage principle," whereby all possible fragment size distributions that satisfy the energy criterion ($\Delta S \leq \Delta S_{critical}$) are considered, can be applied to existing population-balance models of HSG. Since no analytical function exists to accurately and independently predict a breakage pattern, the proposed approach could provide a unique, simple tool and complement existing population-balance models. The proposed model also provides the flexibility to expand its application to granulation processes where more sophisticated granule-fracture modes and binder addition are encountered. The probability of impact and the breakage pattern could also be refined from knowledge of powder and granule flow and impact patterns inside the granulator, if necessary.

This model is particularly useful to understand, control, and scale up processes that are performed in the presence of limited quantities of the binder phase or for scales of operation where the rigor of processing leads to significant granule breakage. The model could also be applied when the binder liquid is introduced as a coarse spray such that the sizes of the nuclei formed by the particles sticking around each droplet are large enough to experience enough kinetic energy of impact under the processing conditions to break apart. Although no attempts were made to independently estimate the parameters, $\Delta S_{critical}$, P, and β, the model could be applied for process prediction or scale-up by defining these parameters a priori through controlled runs with a reference material (or formulation) and at one or more reference scales of operation. The value of $\Delta S_{critical}$ is influenced by the material characteristics that impart granule strength and by the kinetic energy of impact. Hence, a relative measure of hardness (or an alternative strength parameter) of the granules could be used to assign relative values of $\Delta S_{critical}$ to various formulations undergoing HSG. Similarly, although a constant value of β was used for the simulations, in reality, the reattachment of particles to wet crack surfaces could be influenced by the size of the primary particles and the adhesive strength of the binder and would have to be adjusted for each formulation and binder type used. For a given size, the probability of impact, P, is influenced more by the scale of operation and by the design of the granulator equipment than the material characteristics. Hence, a representative value of P could be obtained for a given set of processing equipment and conditions, which then could be applied to various formulations and batches.

In follow-up reports, the parameters P and $\Delta S_{critical}$ would be used to describe and compare between granulator designs, operating conditions, and material properties and to facilitate process scale-up.

CONCLUSIONS

An energy-based model is proposed for high-shear granulation processes, whereby the extent of granule breakage is considered to be directly proportional to the impact-energy and inversely proportional to the strength of the granules. Granule breakage is accompanied by the attachment of powder onto the binder-rich cracked surfaces resulting in granule growth. The importance of factors such as the probability of impact per unit time interval (ie, the rate of impact), the strength of the granules, and the volume of powder that could attach to the binder-rich cracked surface is highlighted by the model and verified by the close correspondence

between the predictions and the experimental results of granule size evolution obtained from granulation experiments run with lactose monohydrate and relatively low amounts of a binder phase comprising polyvinylpyrrolidone and water. This model is particularly useful to understand, control, and scale up processes that are performed in the presence of limited quantities of the binder phase or for scales of operation where the rigor of processing leads to significant granule breakage.

REFERENCES

1. Iveson SM, Litster JD, Hapgood K, Ennis BJ. Nucleation, growth and breakage phenomena in agitated wet granulation processes: a review. *Powder Technol.* 2001;117:3–39.

2. Wehrlé P, Nobelis Ph, Cuiné A, Stamm A. Scaling-up of wet granulation: a statistical methodology. *Drug Dev Ind Pharm.* 1993;19: 1983–1997.

3. Sirois PJ, Craig GD. Scaleup of a high-shear granulation process using a normalized impeller work parameter. *Pharm Dev Tech.* 2000;5:365–374.

4. Litster JD. Scaleup of wet granulation processes: science not art. *Powder Technol.* 2003;130:35–40.

5. Litster JD, Hapgood KP, Michaels JN, Sims A, Roberts M, Kameneni SK. Scale-up of mixer granulators for effective liquid distribution. *Powder Technol.* 2002;124:272–280.

6. Leuenberger H. Scale-up of granulation processes with reference to process monitoring. *Acta Pharm Technol.* 1983;29:274–280.

7. Ameye D, Keleb E, Vervaet C, Remon JP, Adams E, Massart DL. Scaling-up of a lactose wet granulation process in Mi-Pro high shear mixers. *Eur J Pharm Sci.* 2002;17:247–251.

8. Talu I, Tardos GI, Khan MI. Computer simulation of wet granulation. *Powder Technol.* 2000;110:59–75.

9. Faure A, York P, Rowe RC. Process control and scale-up of pharmaceutical wet granulation processes: a review. *Eur J Pharm Biopharm.* 2001;52:269–277.

10. Wauters PAL, Scarlett B, Liu LX, Litster JD, Meesters GMH. A population balance model for high shear granulation. *Chem Eng Commun.* 2003;190:1309–1334.

11. Verkoeijen D, Pouw GA, Meesters GMH, Scarlett B. Population balances for particulate processes: a volume approach. *Chem Eng Sci.* 2002;57:2287–2303.

12. Ramkrishna D, Mahoney AW. Population balance modeling: promise for the future. *Chem Eng Sci.* 2002;57:595–606.

13. McCoy BJ. A population balance framework for nucleation, growth, and aggregation. *Chem Eng Sci.* 2002;57:2279–2285.

14. Hounslow MJ, Ryall RL, Marshall VR. A discretized population balance for nucleation, growth, and aggregation. *AIChE J.* 1988; 34:1821–1832.

15. Liu LX, Litster JD. Population balance modeling of granulation with a physically based coalescence kernel. *Chem Eng Sci.* 2002;57:2183–2191.

16. Maurstad O. *Population Balance Modeling of Agglomeration in Granulation Processes [PhD Thesis]*. [thesis]. Trondheim, Norway: Norges teknisk-naturvitenskapelige universitet (Norwegian University of Science and Technology), Institutt for termisk energi og vannkraft (Department of Thermal Energy and Hydropower); 2002.

17. Immanuel CD, Doyle FJ. Computationally efficient solution of population balance models incorporating nucleation, growth and coagulation: application to emulsion polymerization. *Chem Eng Sci.* 2003;58:3681–3698.

18. Litster J, Ennis B, eds. *The Science and Engineering of Granulation Processes*. Boston, MA: Kluwer Academic Publishers; 2004. Litser J, Ennis B, eds. *Particle Technology Series;* vol 15.

19. Bond FC. Some recent advances in grinding theory and practice. *Brit Chem Eng.* 1963;8:631–634.

20. Bela B. *Principles of Comminution.* Budapest, Hungary: Akadeìmiai Kiadoì; 1964.

21. Plank R, Diehl B, Grinstead H, Zega J. Quantifying liquid coverage and powder flux in high-shear granulators. *Powder Technol.* 2003; 134:223–234.

22. Litster JD, Hapgood KP, Michaels JN, et al. Liquid distribution in wet granulation: dimensionless spray flux. *Powder Technol.* 2001; 114:32–39.